

Tunneling measurements on spin-paired superconductors with spin-orbit scattering

R. Meservey and P. M. Tedrow

Francis Bitter National Magnet Laboratory, Massachusetts Institute of Technology, Cambridge, Massachusetts 02139*

Ronald C. Bruno

Department of Physics, Southern Illinois University, Edwardsville, Illinois 62025

(Received 13 January 1975)

Electron spin effects in superconducting Al films have been studied by measuring the conductance of tunnel junctions in a magnetic field. Superconductor-normal-metal tunnel junctions were made with 50-Å-thick Al and 500–1000-Å-thick Ag films with Al_2O_3 as the barrier. The measured conductance curves were fit by theoretical calculations, which included depairing effects and spin-orbit scattering, and values of the depairing parameter ζ_0 and the spin-orbit parameter b_0 were obtained. The relation $\zeta_0 = \zeta(0) + CH^2/\Delta_0$ was found to describe the (parallel) magnetic field dependence of the depairing. The values of b_0 obtained were independent of H . Superconductor-superconductor tunnel junctions made with two 50-Å-thick Al films were studied with various amounts of Ge and Mn impurities. The Ge impurity simply raised T_c , whereas the Mn lowered T_c and increased b_0 . The approximate dependence of b_0 on the Mn impurity concentration was obtained. The qualitative features for spin-orbit scattering predicted by theory were observed, and spin-flip scattering in the tunneling process was shown to be negligible.

I. INTRODUCTION

The original version of the microscopic theory of superconductivity by Bardeen, Cooper, and Schrieffer¹ (BCS) assumes electron pairing with opposite momentum and opposite spin ($+k\uparrow, -k\downarrow$). Implicit in such pairing are various interesting spin-dependent properties. Yosida² showed that the spin susceptibility goes to zero as the temperature approaches zero. There is an upper limit to the critical magnetic field H_p even for a thin film whose thickness approaches zero, as was shown by Chandrasekhar³ and Clogston.⁴ The quasiparticle density of states splits into separate densities of states for each spin, as was explicitly noted by Fulde.⁵ Sarma⁶ showed that in a parallel magnetic field there is a first-order transition to the superconducting state at low temperatures for films thin enough to approach the paramagnetic limiting field H_p .

Even before the BCS theory was published, Reif⁷ showed that the Knight shift for mercury did not go to zero as the temperature approached zero. Shortly thereafter the same result was obtained for tin,⁸ vanadium,^{9,10} and aluminum.¹¹ Ferrell¹² and Anderson¹³ suggested that the spin-orbit interaction mixed the spin states and that the pairing was between time-reversed states of a more general kind. This theory was further developed by Abrikosov and Gorkov.¹⁴ The combined effect of a magnetic field on electron orbital motion and electron spins in the presence of spin-orbit scattering was worked out by Maki and others.^{15–19} Some paramagnetic limiting of the critical field was shown experimentally in type-II superconductors by Berlincourt, Hake, and

others.^{20–22} However, none of the other predicted properties of a spin-paired superconductor was found.

It was suggested by Bardeen and Schrieffer²³ that if the original BCS pairing was to be found in a superconductor, aluminum was the best candidate because of its small spin-orbit interaction. Measurements of the critical field of thin aluminum films by Strongin and Kammerer²⁴ indicated the effect of spin paramagnetism. Further measurements of aluminum by Hammond and Kelly²⁵ and Fine *et al.*²⁶ showed that the Knight shift approached zero at zero temperature. Measurements by Tedrow, Meservey, and Schwartz²⁷ on ultrathin films of aluminum at temperatures down to 0.4 K definitely established the importance of the paramagnetically limited critical field. In addition, the existence of a first-order phase transition at low temperatures and high fields was deduced from a suppression of fluctuation effects. More recent experiments concerning the critical field of paramagnetically limited aluminum films are summarized in a previous article.²⁸ An article on high-field superconductivity by Fulde reviews theoretical and experimental results on spin effects.²⁹

The present article describes electron tunneling measurements of spin effects in superconductors. The tunneling technique in superconductors, which was introduced by Giaever,³⁰ has been extremely fruitful in the study of superconductors. The energy gap, the superconducting density of states, depairing effects, and the phonon spectrum have all been elucidated by this method. In the study of electron spin effects in superconductors the tunneling method has again proved to be the most informa-

tive technique available. We will describe a number of experiments with both normal-metal-superconductor junctions and superconductor-superconductor junctions. Some of the results have already been briefly reported.³¹⁻³³ It is the present purpose to give a full description of the technique, improve the analysis of the experiments, and give new and more complete results.

II. EXPERIMENTAL PROCEDURES

The tunnel junctions used in this investigation were made in a standard way. First, a very thin ($\approx 50 \text{ \AA}$) Al strip (or Al doped with Ge or Mn) was deposited on a glass substrate cooled to liquid-nitrogen temperature. After the substrate was warmed to room temperature, the film was exposed to air for a few minutes. When the second film was Al or doped Al, the substrate after being returned to vacuum was again cooled to liquid-nitrogen temperature, and the second film (also $\approx 50 \text{ \AA}$ thick) was evaporated across the first. When the second film was Ag, which was deposited in a layer $\approx 1000 \text{ \AA}$ thick, the substrate did not have to be cooled. Solder contacts were evaporated onto the substrate when it had warmed to room temperature.

The junctions were cooled by immersion in liquid ^3He to temperatures down to 0.4 K. The entire cryostat could be rotated to align the films with the magnetic field provided by a horizontal Bitter solenoid with transverse access and a maximum field of 66 kOe.

Most of the data were in the form of X-Y recorder plots of the conductance dI/dV versus voltage V . The conductance g was measured in the usual way using a small ac modulation voltage ($\approx 20 \mu\text{V}$) and a lock-in amplifier (PAR HR-8). Measuring dI/dV in this way has the disadvantage that the measure-

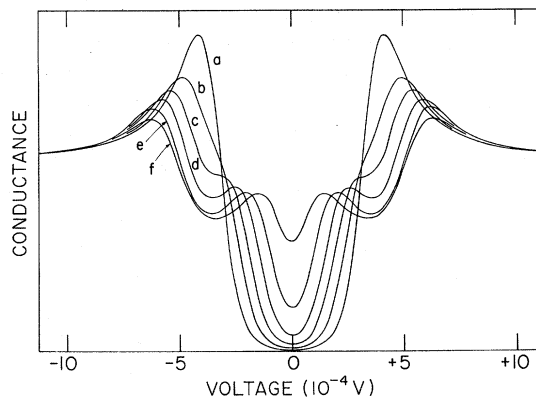


FIG. 1. Conductance vs voltage measurement for an Al-Al₂O₃-Ag tunnel junction at various values of magnetic field H applied parallel to the plane of the films. The symbols on the curves correspond to the values of H in kOe: a=0, b=15, c=22.4, d=29.9, e=37.2, and f=43.1.

ment is not a true four-terminal one, as would be the case in measuring dV/dI . However, since our junctions had fairly high resistances (500–5000 Ω) and the films were either both superconducting or, in the case of Ag, of quite low resistance, the errors introduced by the measurement circuit are small. The advantage of measuring dI/dV is that the data are in a form which can be directly compared with theory without any inversion or other processing. In addition to measuring dI/dV in parallel and perpendicular fields, dc measurements were made of the resistive transition of the films in zero field and of the critical fields at various temperatures. The temperature was measured with a carbon resistance thermometer calibrated against the vapor pressure of ^4He and ^3He .

III. SUPERCONDUCTING-NORMAL-METAL TUNNELING

Figure 1 shows typical measurements of conductance versus voltage for an Al-Al₂O₃-Ag tunnel junction at 0.4 K ($T/T_c \approx 0.16$) for various values of parallel magnetic field H . The Al film is about 50 \AA thick and is therefore thin enough to severely suppress the orbital or Meissner currents so that almost complete paramagnetic limiting is obtained. At zero magnetic field (curve a) we have two conductance peaks separated by approximately the energy gap 2Δ of the superconducting Al. These peaks correspond to the peaks in the density of quasiparticle states and are somewhat rounded by temperature effects. The effect of the magnetic field is apparently to split each of these peaks into two peaks which separate with increasing field. The peak separation is very nearly $2\mu H$ (where μ is the electron magnetic moment) and immediately suggests Zeeman splitting of the quasiparticle states. Such behavior, which has previously been observed,³⁰ can be explained using the BCS model of a superconductor.

A. Comparison with a spin-paired superconductor ($\zeta=0, b=0$)

If we neglect orbital effects (depairing parameter $\zeta=0$) and the effects of spin-orbit interaction (spin-orbit interaction parameter $b=0$) the BCS theory gives for the energy of the quasiparticles

$$E = (\epsilon_k^2 + \Delta^2)^{1/2} ,$$

where ϵ_k is the Bloch-state energy of the quasiparticles, 2Δ is the energy gap, and energy is measured from the Fermi surface. In a magnetic field H , the assumption of opposite-spin electron pairing ($+k\uparrow, -k\downarrow$) leads to a splitting of the quasiparticle energy states,

$$E = (\epsilon_k^2 + \Delta^2)^{1/2} \pm \mu H , \quad (1)$$

where μ is the magnetic moment of the quasiparticles.

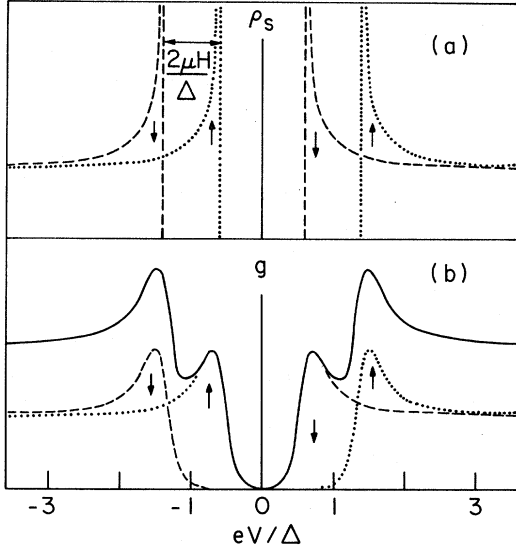


FIG. 2. (a) Theoretical density of states of a BCS spin-paired superconductor in a magnetic field H . Spin-up (dotted) and spin-down (dashed) states are moved up and down, respectively, in energy to give a splitting of $2\mu H$. (b) Corresponding conductance curves at a reduced temperature $t \approx 0.16$ are shown together with the total conductance (solid line).

The quasiparticle density of states $N_s(E)$ according to BCS is

$$N_s(E) = N(0) \frac{\epsilon_k}{(\epsilon_k^2 - \Delta^2)^{1/2}} \equiv N(0)\rho_s, \quad (2)$$

where $N(0)$ is the density of states at the Fermi surface in the normal metal and the normalized BCS density of states ρ_s is defined by Eq. (2). In a magnetic field the quasiparticle distribution is split into two separate spin densities of states

$$N_{s\uparrow} = \frac{1}{2}N(0) \frac{\epsilon_k - \mu H}{[(\epsilon_k - \mu H)^2 - \Delta^2]^{1/2}} \equiv \frac{1}{2}N(0)\rho_{s\uparrow}, \quad (3)$$

$$N_{s\downarrow} = \frac{1}{2}N(0) \frac{\epsilon_k + \mu H}{[(\epsilon_k + \mu H)^2 - \Delta^2]^{1/2}} \equiv \frac{1}{2}N(0)\rho_{s\downarrow}. \quad (4)$$

It is just as if the Fermi energy of the spin-up particles is increased by μH and that of the spin-down particles is decreased by μH . These spin densities of states in a magnetic field are shown in Fig. 2(a).

The tunneling conductance between a superconductor and a normal metal in a magnetic field is likewise composed of spin-up and spin-down parts. Slightly generalizing³⁴ the Giaever model³⁵ of tunneling we obtain, with $\beta = 1/kT$,

$$g(V) = \frac{1}{2} \int_{-\infty}^{\infty} (\rho_{s\uparrow} + \rho_{s\downarrow}) \frac{\beta \exp[\beta(E + eV)]}{\{1 + \exp[\beta(E + eV)]\}^2} dE. \quad (5)$$

Here $g(V) = (dI/dV)_s / (dI/dV)_n$, the differential tunnel

conductance normalized by the conductance with both metals in the normal state. Thus $g(V) = 1$ for H greater than the critical field, and $g(V)$ asymptotically approaches 1 for $eV \gg \Delta$ when $H < H_c$. V is the bias voltage measured from the Fermi energy of the superconductor and e is the absolute value of the electronic charge. The second factor in the conductance integral is a bell-shaped function with half-width β^{-1} symmetrical about $E = -eV$. At $T = 0$ this function degenerates into a δ function and $g(V)$ gives directly the density-of-states function of the quasiparticles. At low but nonzero reduced temperatures the characteristics of ρ_s are still clearly visible, although somewhat rounded by temperature broadening as shown in Fig. 2(b). In this figure the theoretical spin-up (dashed) and spin-down (dotted) conductance curves as well as the total conductance (solid curve) are shown for $T/T_c \approx 0.16$ and $\mu H/\Delta \approx 0.40$.

The theoretical curve 2(b) should correspond to the measured curve labeled d ($H = 29.9$ kOe) in Fig. 1, and in a qualitative way it does. Furthermore, the peaks split as predicted with separation of $2\mu H$ within measurement error, which is about 3%. However, it is immediately apparent that the fit is not exact. The experimental peaks are considerably broader than the theoretical, and this broadening increases with field. Even for $H = 0$ the fit is not exact, as shown in Fig. 3, where the experimental curve (solid line) is compared with the BCS curve (dotted line) for the same values of T and T_c . Therefore it seems appropriate to modify the theory to allow for depairing effects.

B. Effects of pair breaking

Abrikosov and Gorkov¹⁴ (AG) calculated the effect on the superconducting state of low concentrations of paramagnetic impurities. They showed that the presence of paramagnetic impurities dramatically decreases the order parameter and critical temperature. Furthering their analysis, Skalski *et al.*³⁶ showed that magnetic impurities also alter the BCS density of states by rounding off the infinite peak and decreasing the energy gap. The microscopic effect of the magnetic impurities is to break the time-reversal symmetry of the electron states, thus causing the electron pairs to have a finite lifetime. There are other situations in which the time-reversal symmetry of the electron states is broken, as with a uniform transport current, a thin film in a parallel magnetic field, a type-II superconductor in a field, or contact between a superconductor and a paramagnetic film. It has been shown in the short-mean-free-path limit that a single depairing parameter ζ is sufficient to explain all of these effects.^{16, 37-39}

The AG theory gives the order parameter Δ in terms of ζ ,

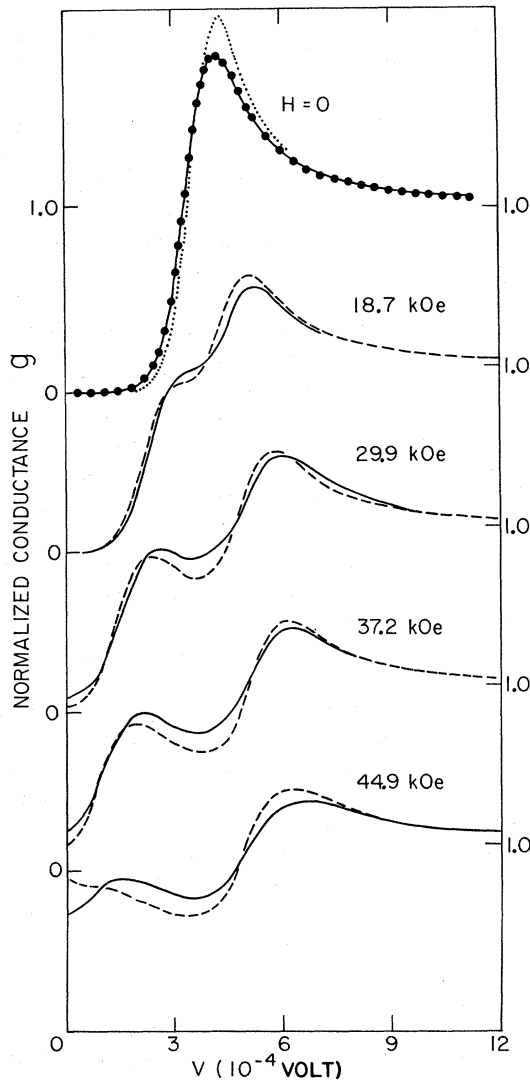


FIG. 3. Normalized conductance g vs voltage at $T/T_c = 0.16$ for five values of magnetic field. The measured curves labeled in kOe are solid lines. For $H=0$ the dotted curve is the BCS theory with $\zeta=0$. The circles are calculated points with $\zeta=0.02$. For $H=18.7, 29.9, 37.2,$ and 44.9 kOe the theoretical curves with $\zeta=0.035, 0.045, 0.06,$ and $0.10,$ respectively, are shown as dashed lines.

$$\ln(\Delta/\Delta_0) = -\frac{1}{4}\pi\zeta \quad \text{for } \zeta \leq 1, \quad (6)$$

where Δ_0 is the order parameter at $T=0$ and $H=0$. At the low reduced temperature ($T/T_c \approx 0.16$) of the present measurements the temperature dependence of Δ is so weak that it can be neglected. The density of states^{16,37} as a function of the electron energy ω for the spin-up and spin-down electrons is

$$N_{\uparrow, \downarrow}(\omega) = \frac{N(0)}{2} \operatorname{Re} \left(\frac{u}{(u^2 - 1)^{1/2}} \right), \quad (7)$$

where u is given by $\omega/\Delta = u[1 - \zeta/(u^2 - 1)^{1/2}]$.

In our experimental situation with thin aluminum films one would expect to observe no depairing at zero magnetic field. Yet when we attempt to fit the experimental conductance using the BCS density of states and $\Delta_0 = 1.76kT_c$ (where T_c is experimentally determined) we find that the theoretical curves have peaks which are too high and too sharply peaked, as shown by the dotted curve in Fig. 3. However, by adding a small amount of depairing we get very good fits to the data. This result is shown in the $H=0$ curve of Fig. 3 for a depairing parameter $\zeta=0.02$, where the theoretical values are shown as points and the measured function is shown as a solid line. The cause of the small depairing at $H=0$ is not known, although any perturbation which breaks the time-reversal symmetry will lead to such depairing.

When a magnetic field is applied to a thin film, Maki and Fulde³⁸ have shown that in the short-mean-free-path limit $l \ll \xi$, which applies to the present experiment, the depairing parameter arising from the orbital motion associated with the finite film thickness d is

$$\zeta = \tau_{tr} (ev_F dH)^2 / 18\Delta. \quad (8)$$

Here τ_{tr} is the transport collision time, v_F is the Fermi velocity, and H is the magnetic field value. The density of states is then both depaired and spin split in this case.

To see how close we could come to explaining the data with such a picture we generated theoretical curves for the given reduced temperature with various values of ζ , displacing them in voltage by $\pm \mu H/e$ and adding them. The curves were normalized by requiring the asymptotic values of $g(V)$ at large absolute values of V to coincide for the experimental and theoretical curves. The value of ζ chosen was that which gave the best over-all fit, with particular emphasis in matching the curvatures near the extrema. Figure 3 shows the chosen theoretical curves (dashed) compared with the experimental curves (solid line) for four values of magnetic field. For all except the highest value of field the theoretical curves follow the measured curves in a general way. However, a consistent deviation is apparent: The theoretical curves are too low near the maximum at the lower voltage. In addition, the splitting of the peaks of the experimental curves appears to be slightly smaller at high fields than predicted by this theory. At the highest field, for which $H=0.86 H_c$, the same behavior is observed, but in addition there is a maximum at $V=0$ instead of a minimum in the theoretical curve; therefore the optimum value of ζ is less certain. On examining Fig. 3 we see that, although the fit is much improved over no depairing, the consistent discrepancy between the theoretical and measured curves suggests that the theory which

does not include spin-orbit effects is not adequate to describe the magnetic field behavior.

The estimates of the depairing parameter ζ when multiplied by the corresponding order parameter Δ should obey an H^2 dependence, as suggested by Eq. (8). Depairing from two different sources will be simply additive, a result which has been derived theoretically by Fulde and Maki¹⁷ and experimentally verified by Guertin *et al.*⁴⁰ Thus it is reasonable to assume that the estimated depairing parameters should just be the sum of the zero-field contribution and the orbital contribution. The data as shown in Fig. 4 can be represented by

$$\zeta(\Delta/\Delta_0) = \zeta_0 + CH^2/\Delta_0, \quad (8)$$

except perhaps at the highest field. We say perhaps because the order parameter Δ is also a function of H , so that near the critical field and particularly if there is a small angular misalignment the value of Δ may be reduced and therefore increase the value of ζ . This could account for the upward trend at the highest field.

C. Effect of spin-orbit interaction

For a spin-paired superconductor with no spin-orbit effects there is Zeeman splitting of the quasiparticle states, as shown in Fig. 5(a).³¹ The BCS density of states is split into a spin-up part and a spin-down part separated in energy by $2\mu H$. Maki⁴¹ considered a thin-film superconductor with spin-orbit scattering centers and showed that in the limit of short electron mean free path the density of states is given by

$$N_{\uparrow\downarrow}(\omega) = \frac{N(0)}{2} \operatorname{Re} \left(\frac{u_{\pm}}{(u_{\pm}^2 - 1)^{1/2}} \right), \quad (9)$$

where u_{\pm} is now defined by

$$\frac{\omega \mp \mu H}{\Delta} = u_{\pm} \left(1 - \frac{\zeta}{(1 - u_{\pm}^2)^{1/2}} \right) + b \left(\frac{u_{\pm} - u_{\mp}}{(1 - u_{\mp}^2)^{1/2}} \right). \quad (10)$$

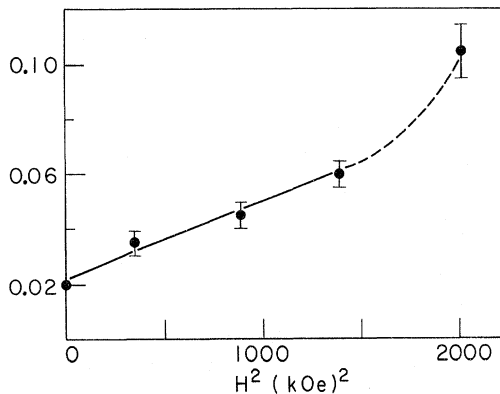


FIG. 4. Depairing parameter ζ obtained from the data of Fig. 3 plotted vs H^2 .

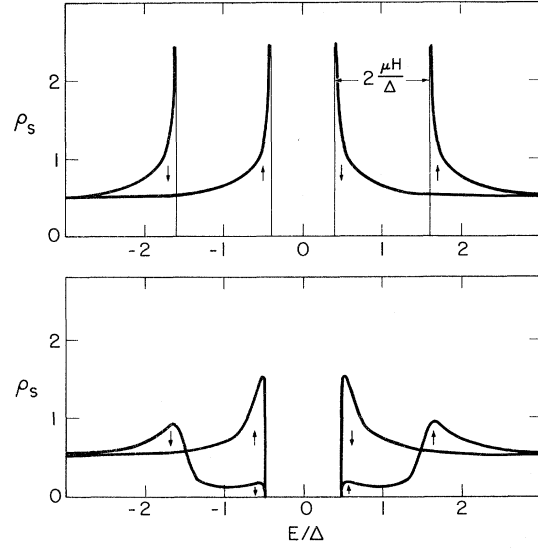


FIG. 5. Theoretical density of states in a magnetic field $H = 0.6\Delta/\mu$. (a) No spin-orbit interaction. (b) Spin-orbit interaction parameter $b = 0.2$.

The spin-orbit scattering parameter is

$$b \equiv \hbar/3\tau_{so}\Delta, \quad (11)$$

and τ_{so} is the spin-orbit scattering time. It is easily seen that at zero magnetic field the density of states is unchanged. However, at finite fields the density of states is split and the states in the two spin directions are partially mixed. Engler and Fulde⁴² have calculated the density of states in a magnetic field; their result for b small but finite is shown in Fig. 5(b). The most striking feature of Fig. 5(b) is that some of the spin states which comprise the peak at large values of $|E|$ are shifted by the spin-orbit interaction to near the peak at low values of $|E|$ and form a small peak just above the energy gap. For larger amounts of spin-orbit scattering this mixing of the spin states increases and the splitting of the peaks decreases until, for $b \rightarrow \infty$, the spin states are completely mixed and the two spin densities of states coalesce into a single density of states identical to that of the BCS theory. Bruno and Schwartz⁴³ have calculated the density of spin states for various values of magnetic field and spin-orbit scattering. The progression of the density-of-states curves for increasing values of b shown in Fig. 6 is from Bruno.⁴⁴ It is evident that the modification of the densities of spin states by including spin-orbit scattering in the theory should improve the agreement with experiment. The general effect is to decrease the magnitude of the higher-voltage peak and to increase that of the lower-voltage peak. In addition the separation of the peaks is decreased.

In Fig. 7 we compare the theoretical predictions,

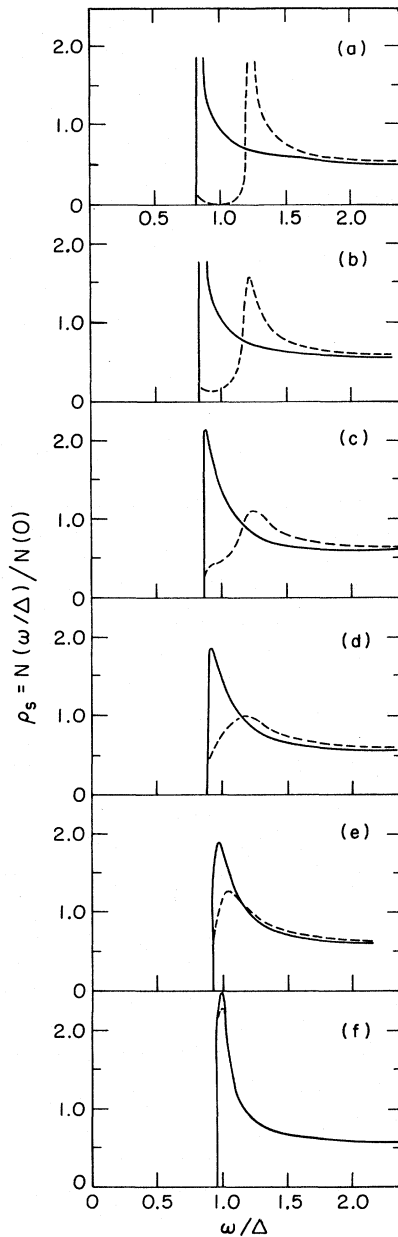


FIG. 6. Theoretical density of states for spin-down (solid line) and spin-up (dashed line) electrons in a magnetic field $H=0.2\Delta/\mu$ with the spin-orbit parameter b as follows: (a) 0.02, (b) 0.1, (c) 0.3, (d) 0.6, (e) 1.5, and (f) 7.0.

including both depairing effects and spin-orbit scattering, with the same experimental results presented in Fig. 3 using the same values of ζ as determined from Fig. 3. The experimental curves are shown as solid lines. The spin-orbit term was determined by assuming values of $b_0 = b(\Delta/\Delta_0) = \hbar/3\tau_{so}\Delta_0$ (that is, $b_0 = b$ for $H=0$) and generating conductance curves for the values of H used in the measurements. The value of b_0 chosen was that

giving the best agreement with the experimental curves. The theoretical curves for $b_0=0.07$ are dashed lines. The fit is very good with the possible exception of the value of g at $V=0$. Adjustments of ζ_0 were attempted to see if better fits would result. In all cases, the values of ζ_0 previously determined were retained even when ζ_0 and b_0 were simultaneously varied in search of the best fit.

After determining b_0 in relatively pure Al films, we attempted to vary the size of b_0 by adding impurities to the film during evaporation. Theoretically, any impurity which is substantially heavier than Al should cause an increase in b_0 . Both Ge and Mn form dilute alloys with Al and have been found to affect the superconducting properties of Al. Either can be added to the Al by simultaneous evaporation from the same crucible, although quantitative control of the percentage of the impurity is difficult. The concentration of Ge used was in the neighborhood of 10 at.%, while that of Mn was less than 0.1 at.%. We have no quantitative way of determining how much Ge was present in the Al films, although work by Hauser⁴⁵ suggests that any Ge in excess of 10 at.% migrates to grain boundaries and has no further effect on the superconductivity. For Mn, on the other hand, we can use the suppression⁴⁶ of T_{c0} as an indicator of how much impurity was added to the Al.

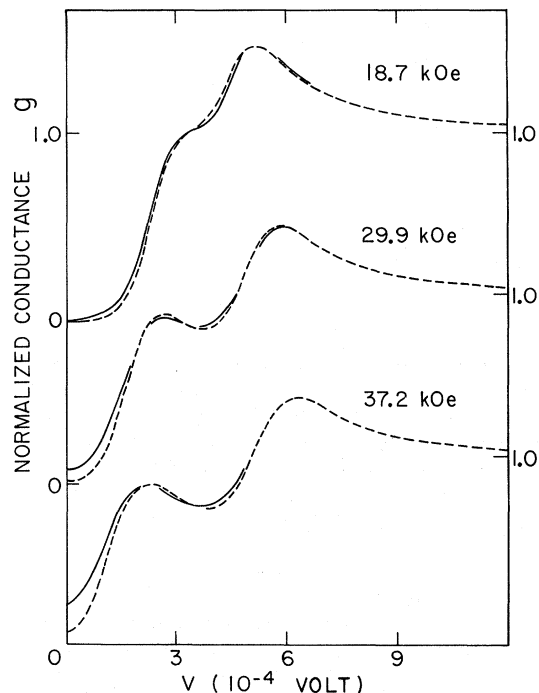


FIG. 7. Comparison of experimental conductance (solid lines) at various values of H with theoretical curves (dashed lines) including depairing (ζ values from Fig. 3) and spin-orbit interaction ($b=0.07$).

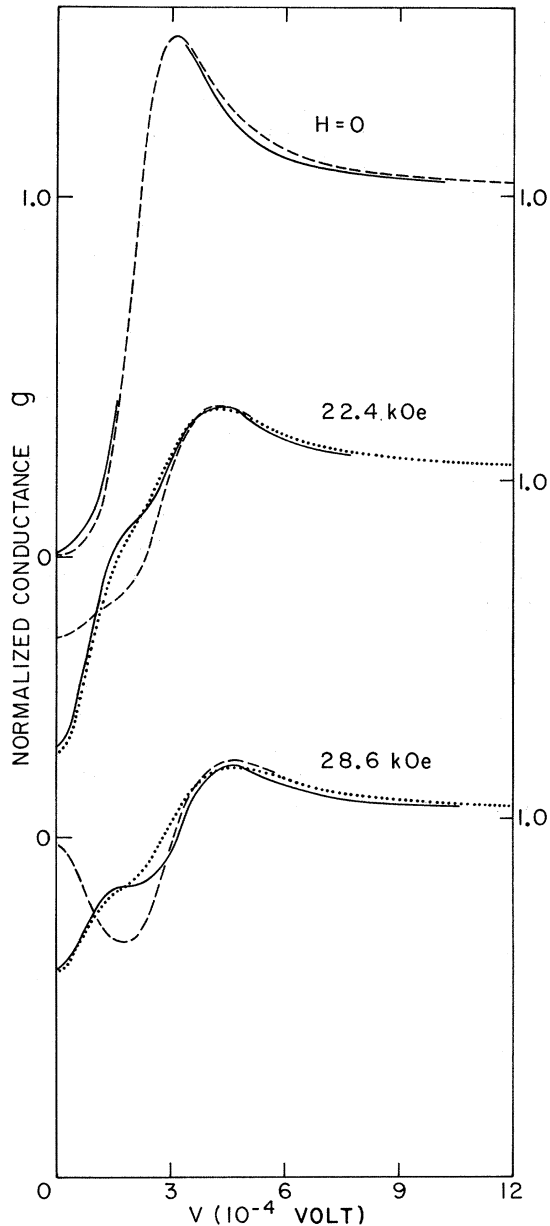


FIG. 8. Comparison of experimental conductance (solid lines) of an Al(Mn)-Ag junction at various values of H with theoretical curves including depairing only (dashed lines) and depairing and spin-orbit interaction (dotted lines). The values of depairing parameter used were $\xi(0)=0.095$, $\xi(22.4)=0.17$, and $\xi(28.6)=0.23$. Spin-orbit parameter $b=0.18$.

Figure 8 shows measured curves (solid lines) of the normalized conductance g as a function of the applied voltage for an Al(Mn)-Ag tunnel junction. The $H=0$ curve is fitted fairly well by a depairing parameter $\xi=0.095$ (shown by dashed curve) which is much greater than that found for pure Al films ($\xi \approx 0.02$). The transition temperature for this

film was 1.84 K, compared with that for pure Al films of the same thickness, which is about 2.5 K. In a magnetic field it is impossible to approximate $g(V)$ using any value of the depairing parameter alone; these theoretical depaired curves are shown as the dashed curves in Fig. 8. Also shown are the calculated curves of $g(V)$ (dotted curves) assuming a spin-orbit parameter $b_0=0.18$ and the depairing parameters given in the figure caption. The fit of the theory to the experimental curve is good and is very sensitive to the value of b_0 , so that the uncertainty in b_0 is only about 5%. Additional tunneling results for impure Al films will be described in Sec. IV.

IV. SUPERCONDUCTOR-SUPERCONDUCTOR TUNNELING

We now consider tunneling measurements between two spin-paired superconductors. If we first neglect the theoretical refinements of depairing and spin-orbit effects, the tunneling behavior in a magnetic field can be deduced from a density-of-states diagram as introduced by Giaever.³⁰ At $H=0$ there will be the usual very sharp maximum in the conductance at $V=\pm(\Delta_1+\Delta_2)/e$ when the filled quasiparticle density-of-states peak of one film has the same energy as the empty peak of the other film. This behavior is shown in the $H=0$ curve of Fig. 9 and differs in no way from the conductance of a non-spin-paired superconductor. In a field the quasiparticle density of states splits into spin-up and spin-down densities of states (Fig. 10), and one might expect some effect on the tunneling curves. However, if spin is conserved in the tunneling process, it is evident that since the densities of states are displaced in voltage by $\pm\mu H/e$ for the two spin directions, and that these displacements are identical for the two films, the over-all tunneling conductance will not be altered by the

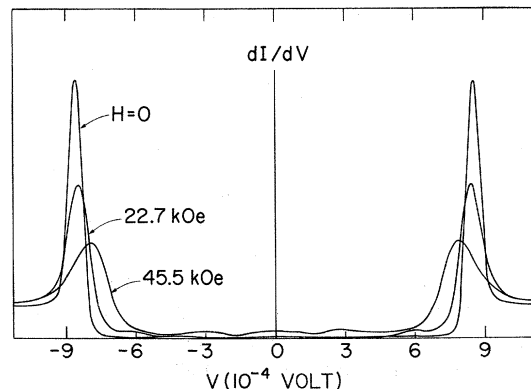


FIG. 9. Conductance of an Al-Al junction in various applied magnetic fields. The peaks at $\pm(\Delta_1+\Delta_2)/e$ are broadened by the field and very small maxima are observed at $\pm(\Delta_1+\Delta_2-2\mu H)/e$.

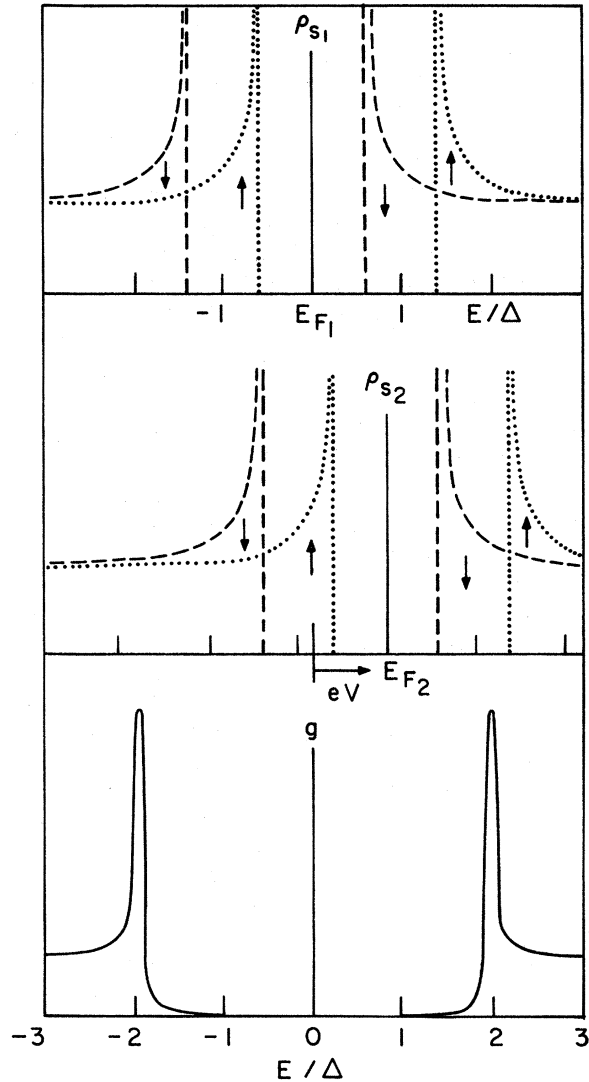


FIG. 10. Densities of states of two identical spin-paired superconducting films in a magnetic field are shown displaced by an amount corresponding to some applied voltage V . When V/e is increased to 2Δ , the quasiparticles can tunnel into states of the same spin and the large conductance peak shown at the bottom is expected in the absence of depairing by the magnetic field.

spin splitting. That is, as long as there is no mixing of the spin states, the peaks in the conductance versus voltage will remain the same independent of the field, and each spin direction will simply contribute one-half of the total conduction. The tunnel current will still be given by the usual expression with the contributions from the two spin directions simply adding. Approximately, this behavior is shown in Fig. 9 at higher fields. There is no obvious splitting of the conductance peaks by the magnetic field. It is true that the single large peak is much broadened at high fields, but this is

mainly caused by the depairing effect of the parallel magnetic field on a film of finite thickness—the same depairing effect that we have seen in superconductor-normal-metal tunneling. If spin were not conserved in the tunneling process, we would expect each of the actually observed peaks to split into three peaks: a large peak in the position of the present peak and two satellite peaks of about one-half the size at $|V| = (\Delta_1 + \Delta_2 \pm 2\mu H)/e$.

Although no such prominent satellite peaks are observed, a careful examination of Fig. 9 shows that there are some very small maxima at $|V| < (\Delta_1 + \Delta_2)/e$ which are field dependent. Figure 11 is a conductance-vs-voltage measurement with much more sensitivity to bring out these small maxima. It was found that these maxima were at voltages $|V| = \Delta_1 + \Delta_2 - 2\mu H/e$. In Fig. 11 the arrows are values of these calculated voltages for each field value and very nearly match the conductance maximum for that field value. Actually, these peaks were only searched for and found after Engler and Fulde⁴² had predicted their presence from a calculation of the spin densities of states of a spin-paired superconductor with some spin-orbit scattering. Figures 5 and 6 show such spin densities of states in a magnetic field. In a qualitative way the most prominent feature is that some of the states in the peak farthest from the Fermi energy are moved toward the Fermi energy and form a small peak near the position of the large peak of the opposite spin. It is easy to see that this sort of density of states gives qualitatively the observed results in which a very small peak is observed at $|V| = (\Delta_1 + \Delta_2 - 2\mu H)/e$, a large peak at $|V| = (\Delta_1 + \Delta_2)/e$, and no peak at $|V| = (\Delta_1 + \Delta_2 + 2\mu H)/e$. This latter peak would only be expected from spin scattering in the tunneling process and not from spin-orbit scattering in the superconductors. Experimental proof of the correctness of this interpretation is given below when supercon-

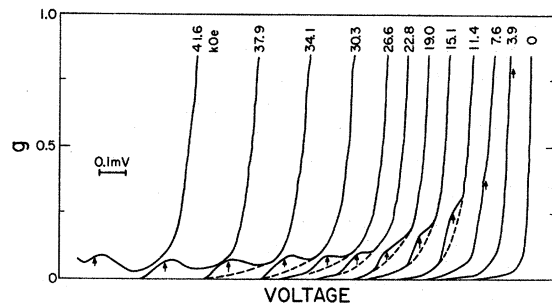


FIG. 11. Expanded plot of g vs V of an Al-Al junction for various applied magnetic fields and for $V < (\Delta_1 + \Delta_2)/e$ showing the peak caused by the mixing of spin states. The arrows mark the position of $V = (\Delta_1 + \Delta_2 - 2\mu H)/e$ for each value of H . The curves have been displaced horizontally for clarity.

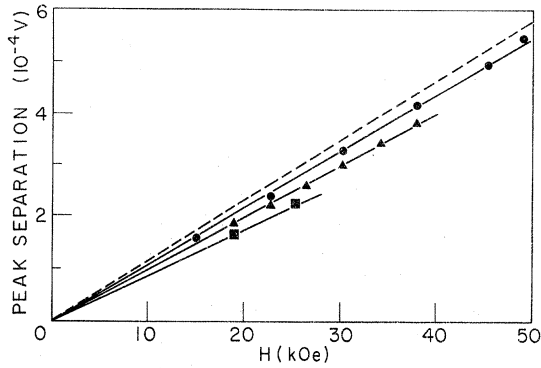


FIG. 12. Voltage separation of the spin-mixing peak and the peak at $(\Delta_1 + \Delta_2)/e$ is plotted against H for Al-Al junctions with various amounts of Mn impurity n in at. %. ●, $T_c = 2.52$, $n = 0.009\%$; ▲, $T_c = 1.85$, $n = 0.06\%$; ■, $T_c = 1.20$, $n = 0.12\%$. The dashed line represents the separation if $b = 0$ in both films.

ductors with more spin-orbit scattering are discussed.

As mentioned previously, tunneling measurements were made with both Ge and Mn as impurities in Al films. Although these spin-orbit effects were observed with both Ge and Mn, the data using Mn are much more complete and we will present them in detail. With Ge, we had difficulty making good tunnel junctions, so $g(V)$ curves were obtained only for a few specimens. The main effect of the Ge is evidently to raise the transition temperature. $H_{c1}(0)$ was raised by about 10%; however, T_{c0} was raised by about the same amount, so that apparently the Ge adds little spin-orbit scattering.

In the case of Mn, the data are much clearer. From the known depression of T_{c0} for bulk specimens we can estimate how much Mn is present in the Al. A number of good tunnel junctions were measured with varying values of T_{c0} and hence varying concentrations of Mn. The increase of the spin-orbit interaction peaks in $g(V)$ with decreasing T_{c0} could be clearly seen. Also, if the voltage difference between the spin-orbit interaction peaks and the $\Delta_1 + \Delta_2$ peaks is plotted versus H , the lower T_{c0} is, the smaller the slope of the resulting straight line, as shown in Fig. 12. Thus, when more Mn is added to the Al, the spin-orbit changes in $g(V)$ become larger and the splitting becomes smaller, in agreement with theoretical expectations. Furthermore, $H_{c1}(t)$ can be fitted theoretically by assuming a larger value of b_0 than is used for pure Al. The experimental evidence shows that b_0 is progressively increased by the addition of Mn.

It is interesting to observe in detail (see Fig. 13) the field-dependent structure for $|V| < (\Delta_1 + \Delta_2)/e$ for a junction with noticeable spin-orbit

scattering caused by Mn impurities ($T_{c0} = 2.52$ K, $b \approx 0.1$). In Fig. 13 $g(V)$ is measured with high sensitivity to show details of the structure. The main peaks in $g(V)$ at $|V| = (\Delta_1 + \Delta_2)/e$ are shown at the sides of the figure to indicate their voltage positions, but the zero of g has been offset to place them in a convenient position. Without this zero offset the $H=0$ main peak would be 1.75 times the height of the figure. As H increases, the spin-orbit peak moves away from the position of the corresponding main peak to lower voltages. At 49.27 kOe these peaks are designated a , a' in the figure. The peaks b , b' closer to the origin of this same curve are the difference peaks $(\Delta_1 - \Delta_2)/e$ of the two Al(Mn) films. The films have slightly different order parameters because of slightly different thickness. The transition temperature of Al films decreases as the thickness increases, so

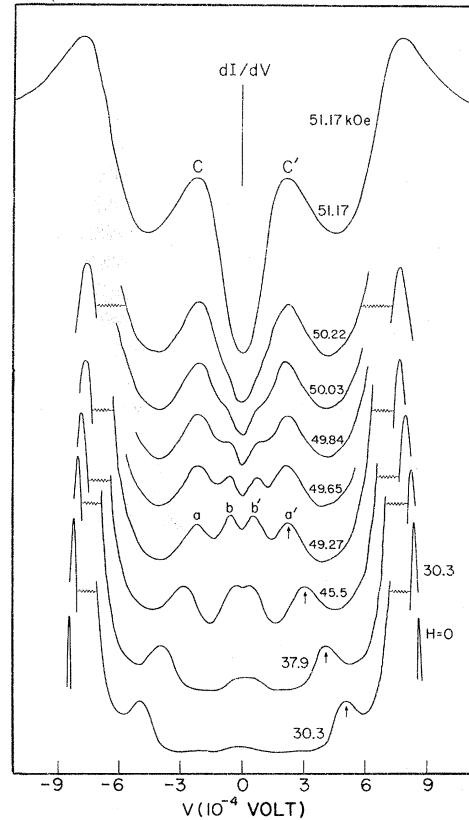


FIG. 13. Magnetic field dependence of the structure of dI/dV for an Al(Mn)-Al(Mn) junction as H approaches H_c . The peaks aa' are due to spin mixing, while bb' are the usual maxima which occur at $V = \pm(\Delta_1 - \Delta_2)/e$. The maxima at $V = \pm(\Delta_1 + \Delta_2)/e$ are shown displaced vertically for reference. With $H = 51.17$ kOe, film 2 is normal and the maxima cc' are the spin-split peaks described earlier for normal-metal-superconducting tunneling. The arrows mark the points used in making the plot of Fig. 14. The curves have been displaced vertically for clarity.

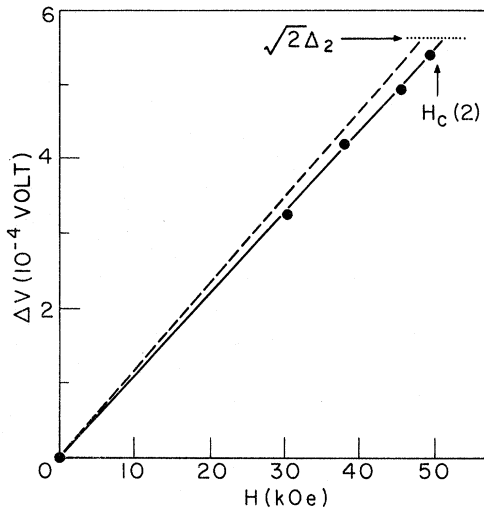


FIG. 14. Plot similar to Fig. 12 for the junction of Fig. 13. The dashed line indicates expected behavior for superconductors with $b=0$. The critical field $H_{c(2)}$ of the thicker film is indicated, along with the voltage separation ΔV at which $\Delta V = \sqrt{2}\Delta(0)/e$.

that in a magnetic field the difference $\Delta_1 - \Delta_2$ increases, since for the thicker film (with the smaller order parameter) Δ_2 will decrease more rapidly than Δ_1 . As H approaches the critical field of the thicker film $H_{c(2)} \approx 50.5$ kOe, the difference peak at $(\Delta_1 - \Delta_2)/e$ merges into the spin-orbit peak at $(\Delta_1 + \Delta_2 - 2\mu H)/e$ at a field of 50.22 kOe. By a field of 51.17 kOe the thicker film is completely normal and we have the usual split peaks of superconductor-normal-metal tunneling where the outer peaks are at $\pm(\Delta_1 + \mu H)/e$ and the inner peaks (designated by c, c') are at $\pm(\Delta_1 - \mu H)/e$. The sharpness of the transition between the two tunnel-

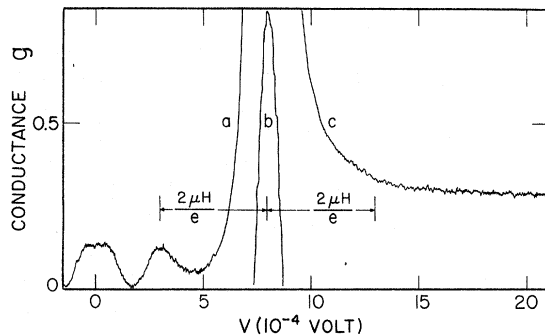


FIG. 15. Conductance g vs V for the same junction as in Fig. 13. The peak at $V = (\Delta_1 + \Delta_2)/e$ (labeled b) has been displaced downward by 2.45 (in units of the normal-state conductance), while the portion labeled c has been displaced downward by 0.73 units. The absence of a peak at $V = (\Delta_1 + \Delta_2 + 2\mu H)/e$ shows that spin flipping does not take place during tunneling.

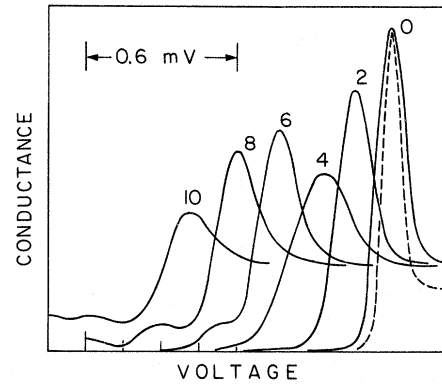


FIG. 16. Conductance of an Al(Mn)-Al(Mn) junction for several values of magnetic field. In low H (curves 0, 2, 4) the conductance peak at $V = (\Delta_1 + \Delta_2)/e$ is quite broad. In higher fields (curves 6, 8, 10) the peak becomes sharper and the spin-orbit interaction peak appears. The curves have been displaced horizontally. The value of H in kOe for each curve can be found by multiplying the number of the figure by 3.79.

ing modes shows strikingly the first-order transition of the thicker film and is characteristic of spin-paired superconductors.

In Fig. 14 we plot the voltage difference ΔV between the main peak and the spin-orbit peak as a function of H to within 96% of $H_{c(2)}$, the critical field of the thicker film. The measured values of ΔV as a function of H (the points and solid line of Fig. 14) are only slightly less than $\Delta V = 2\mu H/e$ (shown by the dashed line), to be expected for superconducting films with $b=0$. The critical field of a perfectly spin-paired superconductor is predicted to be $H_p = \Delta_0/(2\mu)^{1/2}$ and the corresponding value of $\Delta V = 2\mu H_p/e = (2\Delta_0)^{1/2}/e$. To apply this result in the present case we obtain Δ_2 from Fig. 13. Taking $(\Delta_1 + \Delta_2)/e$ to be given by the main peak at $H=0$ and $(\Delta_1 - \Delta_2)/e = \frac{1}{2}(V_b - V_b)$ we obtain a value of Δ_2 . The theoretical maximum value of ΔV corresponding to H_p is then $\sqrt{2}\Delta_2/e$, as shown in Fig. 14, and the critical field of the thicker film $H_{c(2)}$ is only 2% greater than predicted by perfect spin pairing. Thus, although the effect of the spin-orbit parameter b is clearly visible, the films are still acting like nearly perfectly spin-paired superconductors.

The normalized conductance $g(V)$ of this same junction is shown in Fig. 15 for higher values of V . This measurement is a particularly clear demonstration that the additional peak at $|V| = (\Delta_1 + \Delta_2 - 2\mu H)/e$ is due to spin-orbit effects and not to mixing of the spin states during the tunneling process. This last mechanism would produce a peak $|V| = (\Delta_1 + \Delta_2 + 2\mu H)/e$. The absence of such a peak is very clear in this example.

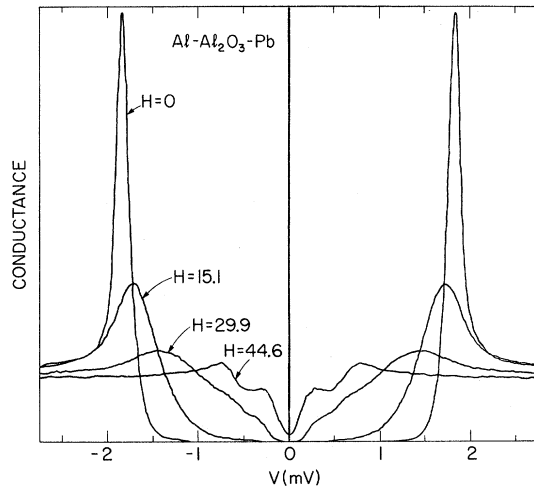


FIG. 17. Conductance of an Al-Pb tunnel junction in various applied magnetic fields.

Although the behavior of Al(Mn) junctions is well explained by an increased value of b , unfortunately the Al-Mn system⁴⁶ is not a simple one. Small concentrations of Mn lower T_{c0} for Al even faster than do such ferromagnets as Fe and Co. There is apparently some interaction between the conduction electrons of Al and the $3d$ levels of the Mn that is not well understood, but which can be described in terms of localized spin fluctuations. That the behavior of Mn in Al is not simple is demonstrated by the tunneling conductance curves for one particular Al(Mn)-Al(Mn) junction shown in Fig. 16. Curves of $g(V)$ versus V are shown for various applied H . For small H the peaks in g at $\pm(\Delta_1 + \Delta_2)/e$ are quite broad and grow increasingly broad as H increases. Also, there is no evidence of the spin-orbit interaction peaks. At a certain field, the peaks become suddenly narrower and the spin-orbit interaction peaks appear. Thus in this film the Mn is acting like a magnetic scatterer at low fields, causing spin-flip scattering⁴³ and consequent broadening of $g(V)$. At higher fields the scatterers become aligned and can no longer flip their spins, so the scattering becomes of the spin-orbit type. Unfortunately, although the experimental result is very clear, we were not able to reproduce this effect in other junctions. Further investigation of this effect requires close control of the Mn concentration, and further study of the transition was not undertaken at this time.

A heavy superconductor such as Pb is expected theoretically¹⁴ to have a large value of b . Knight-shift measurements have been consistent with this expectation.^{7-11,25,26} The tunneling technique de-

scribed in this paper is a simple method of determining the value of b in various superconductors, provided only that the metals can be prepared in the form of very thin continuous films. With Al such preparation is simple. With most other superconductors it is difficult, due mainly to agglomeration and oxidation. We attempted to measure b for Pb by the tunneling technique, but have been only marginally successful. The thinnest Pb film we could make and measure was 140 Å thick, which is not thin enough to reduce orbital effects to a level sufficiently low that mainly spin effects remain. The resulting g -vs- V curves for a Al-Al₂O₃-Pb junction are shown in Fig. 17. At low fields, the only noticeable feature is the large peak at $|eV| = \Delta_{Al} + \Delta_{Pb}$. This peak moves to lower voltages and broadens because of depairing and because Δ_{Pb} decreases as the field increases. The broadening might also be caused by splitting of the peak in the magnetic field, which is the expected behavior if b is large in Pb. (Note that if the density of states of Pb does not split, the tunneling conductance should show the splitting of the Al density of states. If the Pb density of states is split by an amount $2\mu H$ no splitting should be detected in the tunneling conductance.) As H is increased further, a shoulder develops near zero voltage which grows into the split Al-normal-metal conduction as the Pb film is driven normal by the field. The final result is ambiguous, but the lack of a definite spin splitting in the $H = 15.1$ kOe curve implies that b may not be as high as one would predict for Pb. Further measurements are necessary to clarify this point.

V. SUMMARY

We have shown that the shape of the tunneling-conductance-vs-voltage curves of Al-Al₂O₃-Ag junctions in a magnetic field can be explained in detail when both depairing and the spin-orbit interaction are taken into account.

Adding Mn impurities to the Al to increase the value of the spin-orbit scattering parameter b_0 up to 0.18 changes the shape of the tunneling curves in the way expected from the theory. In Al-Al₂O₃-Al superconducting-superconducting tunnel junctions the effects of spin mixing of the quasiparticle states are dramatic and can be explained in detail. The expected decrease in the Zeeman splitting with increased values of b_0 was observed. Another property of paramagnetically limited superconductors, the first-order phase transition at low T and high H , is clearly demonstrated by the field dependence of the tunneling conductance of these junctions. Attempts to extend this study to other superconductors was only marginally successful and more investigation is needed for superconductors with large spin-orbit scattering.

- *Supported by the National Science Foundation.
- ¹J. Bardeen, L. N. Cooper, and J. R. Schrieffer, *Phys. Rev.* **108**, 1175 (1957).
 - ²K. Yosida, *Phys. Rev.* **110**, 769 (1958).
 - ³B. S. Chandrasekhar, *Appl. Phys. Lett.* **1**, 7 (1962).
 - ⁴A. M. Clogston, *Phys. Rev. Lett.* **9**, 266 (1962).
 - ⁵P. Fulde, *Solid State Commun.* **5**, 181 (1967).
 - ⁶G. Sarma, *J. Phys. Chem. Solids* **24**, 1029 (1963); K. Maki and T. Tsuneto, *Prog. Theor. Phys.* **31**, 945 (1964).
 - ⁷F. Reif, *Phys. Rev.* **106**, 208 (1957).
 - ⁸G. M. Androes and W. D. Knight, *Phys. Rev.* **121**, 779 (1961).
 - ⁹R. J. Noer and W. D. Knight, *Rev. Mod. Phys.* **36**, 177 (1964).
 - ¹⁰A. M. Clogston, A. C. Gossard, V. Jaccarino, and Y. Yafet, *Phys. Rev. Lett.* **9**, 262 (1962).
 - ¹¹R. H. Hammond and G. M. Kelly, *Rev. Mod. Phys.* **36**, 185 (1964).
 - ¹²R. A. Ferrell, *Phys. Rev. Lett.* **3**, 262 (1959).
 - ¹³P. W. Anderson, *Phys. Rev. Lett.* **3**, 325 (1959).
 - ¹⁴A. A. Abrikosov and L. P. Gorkov, *Zh. Eksp. Teor. Fiz.* **42**, 1088 (1962) [*Sov. Phys.-JETP* **15**, 752 (1962)].
 - ¹⁵K. Maki, *Phys. (N. Y.)* **1**, 127 (1964).
 - ¹⁶K. Maki and T. Tsuneto, in Ref. 6.
 - ¹⁷P. Fulde and K. Maki, *Phys. Rev.* **141**, 275 (1966).
 - ¹⁸N. R. Werthamer, E. Helfand, and P. C. Hohenberg, *Phys. Rev.* **147**, 295 (1966).
 - ¹⁹K. Maki, *Phys. Rev.* **148**, 362 (1966).
 - ²⁰T. G. Berlincourt and R. R. Hake, *Phys. Rev.* **131**, 140 (1963).
 - ²¹Y. B. Kim, C. F. Hempstead, and A. R. Strand, *Phys. Rev.* **139**, A1163 (1965).
 - ²²R. R. Hake, *Phys. Rev. Lett.* **15**, 865 (1965); *Appl. Phys. Lett.* **10**, 189 (1967); *Phys. Rev.* **158**, 336 (1967).
 - ²³J. Bardeen and J. R. Schrieffer, in *Progress in Low Temperature Physics*, edited by C. J. Gorter (North-Holland, Amsterdam, 1961), Vol. 3, p. 170.
 - ²⁴M. Strongin and O. F. Kammerer, *Phys. Rev. Lett.* **16**, 456 (1966).
 - ²⁵R. H. Hammond and G. M. Kelly, *Phys. Rev. Lett.* **18**, 156 (1967).
 - ²⁶H. L. Fine, M. Lipsicas, and M. Strongin, *Phys. Lett.* **29**, A366 (1969).
 - ²⁷P. M. Tedrow, R. Meservey, and B. B. Schwartz, *Phys. Rev. Lett.* **24**, 1004 (1970).
 - ²⁸P. M. Tedrow and R. Meservey, *Phys. Rev. B* **8**, 5098 (1973).
 - ²⁹P. Fulde, *Adv. Phys.* **22**, 667 (1973).
 - ³⁰I. Giaever, *Phys. Rev. Lett.* **5**, 464 (1960). For a recent review of the literature see L. Solymar, *Superconducting Tunneling and Applications* (Wiley, New York, 1972).
 - ³¹R. Meservey, P. M. Tedrow, and P. Fulde, *Phys. Rev. Lett.* **25**, 1270 (1970).
 - ³²P. M. Tedrow and R. Meservey, *Phys. Rev. Lett.* **27**, 919 (1971).
 - ³³R. Meservey, in *Proceedings of the Thirteenth International Conference on Low Temperature Physics*, edited by K. D. Timmerhaus, Q. J. O'Sullivan, and E. F. Hammel (Plenum, New York, 1974), Vol. 3, pp. 345-353.
 - ³⁴P. M. Tedrow and R. Meservey, *Phys. Rev. B* **7**, 318 (1973).
 - ³⁵I. Giaever and K. Megerle, *Phys. Rev.* **122**, 1101 (1961).
 - ³⁶S. Skalski, O. Betbeder-Matibet, and P. R. Weiss, *Phys. Rev.* **136**, A1500 (1964).
 - ³⁷K. Maki, *Prog. Theor. Phys.* **31**, 731 (1964).
 - ³⁸K. Maki and P. Fulde, *Phys. Rev.* **140**, A1586, (1965).
 - ³⁹P. Fulde, in *Tunneling in Solids*, edited by E. Burstein and S. Lundquist (Plenum, New York, 1969), p. 429.
 - ⁴⁰R. P. Guertin, W. E. Masker, T. W. Mihalisin, R. P. Groff, and R. D. Parks, *Phys. Rev. Lett.* **20**, 387 (1968).
 - ⁴¹K. Maki, *Prog. Theor. Phys.* **32**, 29 (1964).
 - ⁴²H. Engler and P. Fulde, *Z. Phys.* **247**, 1 (1971).
 - ⁴³R. Bruno and B. B. Schwartz, *Phys. Rev. B* **8**, 3161 (1973).
 - ⁴⁴R. Bruno, thesis (MIT, 1972) (unpublished).
 - ⁴⁵J. J. Hauser, *Phys. Rev. B* **3**, 1611 (1971).
 - ⁴⁶E. Babic, P. J. Ford, C. Rizzuto, and E. Salamoni, *J. Low Temp. Phys.* **8**, 219 (1972); G. Boato, G. Gallinaro, and C. Rizzuto, *Phys. Rev.* **148**, 353 (1966).